Phys. Status Solidi C **9**, No. 6, 1361–1365 (2012) / **DOI** 10.1002/pssc.201100534

physica status solidi c
www.pss-c.com
current topics in solid state physics

Adsorption of OH and H at the $LiNbO_3$(0001) surface

R. Hölscher, S. Sanna*, and W. G. Schmidt

Lehrstuhl für Theoretische Physik, Universität Paderborn, 33098 Paderborn, Germany

Received 2 September 2011, revised 19 October 2011, accepted 19 October 2011
Published online 20 February 2012

Keywords theory, DFT, adsorption, $LiNbO_3$, surfaces

* Corresponding author: e-mail simone.sanna@uni-paderborn.de, Phone: +49-(0)5251-602324, Fax: +49-(0)5251-603435

The adsorption of single hydrogen atoms and hydroxyl radicals (OH) at the polar (0001) surface is simulated by means of *first-principles* total energy calculations, in order to investigate the influence of ferroelectric poling on the surface physics and chemistry of $LiNbO_3$. H and OH are found to adsorb at a similar site both at the positive and at the negative (0001) surface. Despite this, the adsorption energy is for both adsorbates strongly polarization dependent, with adsorption energy differences as high as 2 eV. This striking contrast is traced back to electrostatic effects, which lead to a different bonding scenario at the two LN(0001) sides. The polar radical OH lies relatively flat on the positive surface, with the adsorbate oxygen forming a covalent bond with the surface oxygen. At the negative face, OH adsorbs roughly perpendicular and the adsorbate oxygen forms a bond of covalent nature with the surface cations. The adsorbate dipole moment is directed against the spontaneous polarization of the substrate.

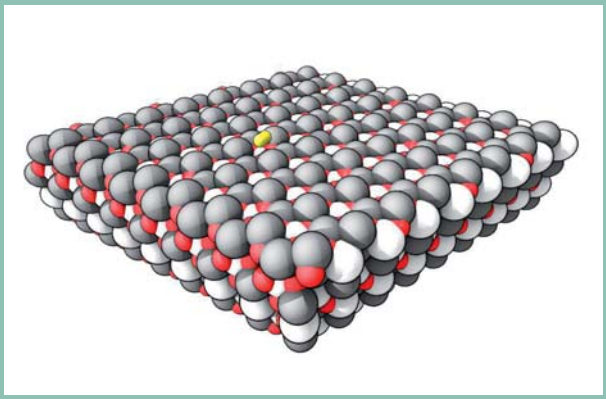

(Color online) OH radical adsorbed at the $LiNbO_3$ (0001) positive surface (perspective view). White atoms are Nb, gray atoms Li and red atoms O.

1 Introduction Lithium niobate ($LiNbO_3$, LN) is a ferroelectric material frequently used for various (nonlinear) optical and acoustic applications [1,2]. While traditional applications mainly exploit LN bulk properties, more recently the (microscopic) surface and interface properties have become important [3]. In particular, the polarization domains of ferroelectric surfaces can be manipulated by an external electric field in order to tailor the surface reactivity for specific applications. Indeed, polarization-dependent physical and chemical surface phenomena have been reported. Surface conductivity [4], threshold energy for photoelectron emission [5], thermally stimulated electron emission [6] and etching rate in acid solutions [7,8] have shown to be very different for differently polarized domains. Polarization-dependent adsorption of particle and molecules, either directly on the ferroelectric surface [9,10] or on metal and semiconducting thin films [11] deposited in a ferroelectric support, have been demonstrated too. Furthermore, photochemical deposition reactions can be combined with the local control of the ferroelectric polarization to drive the assembly of surface nanostructures [12]. Recently, it has been suggested that molecular adsorption may stabilize opposite poling directions in ferroelectric thin films, allowing for the realization of ferroelectric chemical sensors [13]. Due to this interesting possibilities, different studies have been

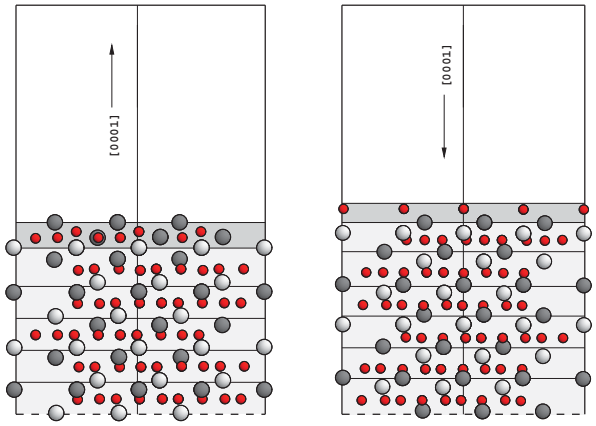

Figure 1 (Color online) Side view of the slab used to model the adsorption at the positive (left hand side) and negative (right hand side) $LiNbO_3$ (0001) surface. The -Nb-O_3-Li- trilayers and the surface termination (-Nb-O_3-Li_2 for the positive side and O-Li- for the negative side) are indicated. White atoms are Nb, gray atoms Li and small atoms O.

dedicated to the understanding of the mechanisms behind the polarization-dependent interaction between adsorbates and surfaces. These include the photochemical deposition of metal nanoparticles [14,15], deposition of charged particles [16] and the adsorption and reaction of molecules on different ferroelectric surfaces [9,17,18]. These studies yield to a rather complicated picture, in which many factors such as internal and external screening charges on the surfaces, electrostatic forces induced by space charge layers, pyroelectric and piezoelectric effects, and charge transfer processes contribute to the observed polarization dependence of the adsorption. These contributions depend, in turn, on the particular ferroelectric surface (electronic carrier density, electronic band gap, presence of defects and domain boundaries) on its preparation (sample thickness, polishing, annealing temperature) and on the experimental setup (substrate temperature, environment composition and pressure, light source used for the carrier excitation). In the case of lithium niobate the stoichiometry and the morphology of differently polarized clean surfaces are known to be different [19–23], too. In the present manuscript we study the adsorption of hydrogen atoms and hydroxyl radicals at the positive and negative LN(0001) surface by means of atomistic simulations in the framework of the density functional theory (DFT). Adsorption energy, site and configuration are determined and the bond with the two surfaces analyzed and discussed. This allows us both to understand the different mechanisms underlying the interaction of these common adsorbates with differently polarized surfaces and represents, at the same time, the first step towards the investigation of water adsorption and surface etching.

2 Methods Total energy density functional calculations have been performed within the PW91 formulation of the generalized gradient approximation (GGA) [24] as implemented in the VASP simulation package [25]. PAW potentials [26] with projectors up to $l = 3$ for Nb, $l = 2$ for Li, O and $l = 1$ for H have been used for the calculations. The electronic wave functions are expanded into plane waves up to a kinetic energy of 400 eV. Our work is based on the stable surface models proposed in [21,22], which are in accord with the experimental observation. According to this model, the positive surface is -Nb-O_3-Li_2 terminated, with one of the two top Li atoms relaxing down to the lower laying oxygen layer and the other above it, as represented in Fig. 1 and Fig. 2a. The negative surface is -Li-O terminated, instead (see Fig. 1 and Fig. 2b). These geometries are used as basis for the investigation of the H and OH adsorption. Thereby we use slabs consisting of 18 atomic layers within a 2×2 periodicity (124 atoms for the positive face and 128 for the negative) and a vacuum region of ca. 16 Å. Both slabs are represented in Fig. 1. The lateral repetition drastically reduces the spurious interaction between the charged adsorbates and their periodic images in neighboring supercells. Using one molecule per slab (which is a rhombus with diagonals of 10.32 Å and 17.88 Å in the XY-plane) corresponds, in first approximation, to the zero-coverage adsorption (or desorption) mentioned, for example, in [10]. Higher coverages are not investigated in this work. The dipole correction described in [27,28] has been used to correct the artificial forces generated by the slab images. A Γ-centered $2\times2\times1$ k-point mesh was used to carry out the integration in the Brillouin zone. The adsorbate and up to 12 uppermost surface layers were allowed to relax until the forces acting on each atom were lower than 50 meV/Å.

3 Results We started our investigation with the determination of the favored adsorption site for H atoms and for the OH radicals on the considered model structure. We follow Ref. [1,21,22] concerning the convention for discriminating positive and negative surfaces, which differs from Ref. [10]. In a first step we have calculated the potential energy surface (PES) for single adsorbates, which gives an approximate idea of the stable adsorption site and a map of the different energy minima on the surface. The PES is calculated constraining the lateral coordinates of the lower atom of the adsorbate and allowing the remaining degrees of freedom and the uppermost six substrate layer to relax. We have evaluated the adsorption energy for 48 possible positions, and three different starting configuration in the case of OH adsorption. The results are reported in Fig. 2 and Fig. 3 for the adsorption of H and OH, respectively. The PES for the adsorption of H at the negative side (Fig. 2b) is much more corrugated than in the case of the positive side (Fig. 2.a), indicating a lower surface mobility of the adsorbate. Several minima and maxima of the adsorption energy are present at both sides. As a general

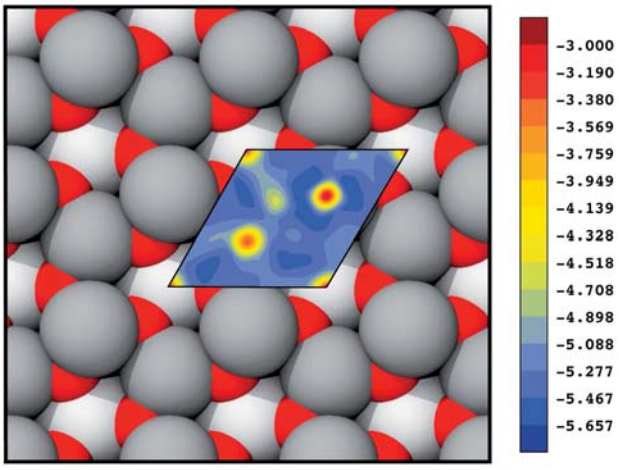

a) Positive $LiNbo_3$ surface.

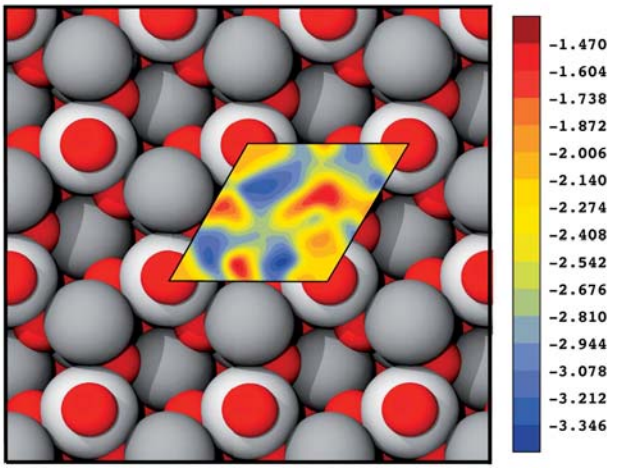

b) Negative $LiNbO_3$ surface.

Figure 2 (Color online) Potential energy surface for the adsorption of a single H atom on the $LiNbO_3(0001)$ surface. Li atoms are gray, Nb white and oxygen red. Adsorption energies are in eV.

feature, H avoids a position right on top of the topmost Li (positive side) and Li,O (negative site) atoms, and prefers an adsorption site betwen cations, above the lower laying oxygen atoms. The PES for the adsorption of OH (Fig. 3) shows similar features, even if the difference in the ion mobility at the two sides is not so pronounced as for hydrogen.

In a second step, we have determined the optimal configuration for the adsorption of a single H atom or OH molecule. Thereby, we start with the adsorbate in several of the favored adsorption sites as obtained from the PES calculation. However, we now let the molecule and the surface relax without any constraints. Neither H atoms nor OH molecules considerably move toward other adsorption sites, indicating that the mesh used for PES calculation was fine enough. In the relaxed geometry, H results bound with an oxygen atom at the positive site and a Li atom at the negative side, with a bond length of 0.99 Å and 1.8 Å, respectively. In both cases the hydrogen adsorption causes some rearrangement of the surface atoms.

The adsorbed OH molecule lays relatively flat on the positive surface, with the oxygen bound to a surface oxygen at a distance $d(\mathrm{O}-\mathrm{O}) = 1.49$ Å. The electronic charge redistribution upon adsorption is shown in Fig. 4a. Charge isolines are represented in a plane parallel to the crystal c-axis and containing the adsorbate and the surface oxygen. An important fraction of the electronic charge is localized between the two oxygen atoms. This charge distribution, together with the O-O interatomic distance (the covalent radius of oxygen is 0.73 Å) suggests a covalent bond between surface and adsorbate. On the negative surface the molecule is roughly perpendicular to the surface, instead, and located between a Li $d(\mathrm{O}-\mathrm{Li}) = 1.84$ Å and a Nb atom $d(\mathrm{O}-\mathrm{Li}) = 2.08$ Å, as plotted in Fig. 4b. An analysis of the charge distribution shows electronic charge accumulation close to the adsorbate oxygen and depletion close to the Nb atom as expected for a ionic interaction, while the Li atom seems not to be affected by the presence of the adsorbate. The polarization of the molecule is directed against the spontaneous polarization of the material. As for H, the presence of the adsorbate induces some relaxation of the surface atoms.

The adsorption energy, as calculated from the difference

$$E_{\mathrm{ads}} = E_{\mathrm{slab}}(\mathrm{Ads@LN}) - E_{\mathrm{slab}}(\mathrm{LN}) - \mathrm{E}_{\mathrm{free}}(\mathrm{Ads}) \tag{1}$$

amounts to 6.0 and 3.8 eV for the hydrogen adsorption at the positive and negative surface respectively, and 2.9 and 5.7 eV for the OH molecule. The adsorption energy for H is higher at the positive surface than at the negative surface, while for OH molecules the adsorption at the negative side is favored. The high adsorption energy is expected for extremely reactive substances as hydrogen and hydroxyl radicals, however the pronounced plarization dependence is, at a first sight, surprising. This can be understood, however, by simple electrostatic considerations. Both hydrogen and OH radicals posses one unpaired electron. While OH reaches a stable configuration by capturing one electron (OH^-, hydroxide), hydrogen acts as a donor. Capturing an electron from the positive surface further increases the surface charge (e.g. makes it even more positive), while subtracting an electron from the negative side stabilizes it. This explains why the OH adsorption at the negative side is favored with respect to the adsorption at the positive side. Vice versa, the adsorption of hydrogen atoms has a stabilizing effect at the positive surface. Unfortunately, no experimental data are available, which can be directly compared with our calculations.

4 Conclusions We have performed density functional calculations to simulate the effect of ferroelectric poling on the chemical properties of lithium niobate sur-

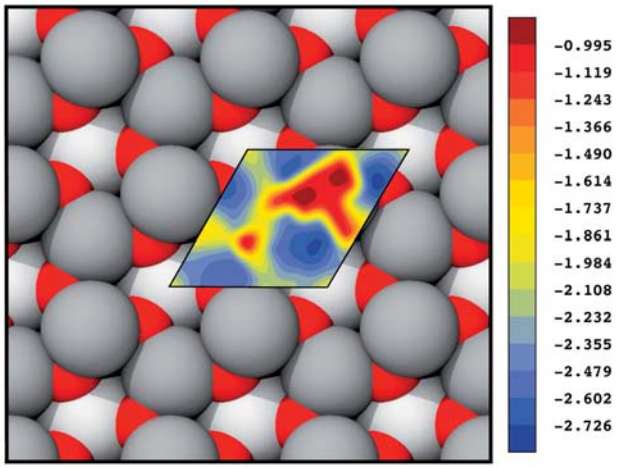

a) Positive $LiNbO_3$ surface.

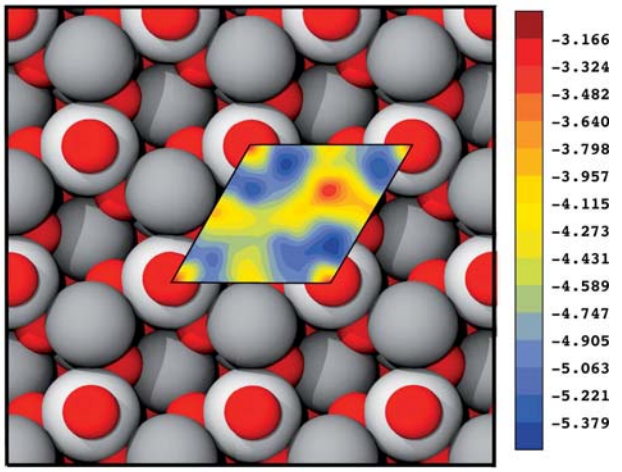

b) Negative $LiNbO_3$ surface.

Figure 3 (Color online) Potential energy surface for the adsorption of a single OH molecules on the $LiNbO_3$(0001) surface. Li atoms are gray, Nb white and oxygen red. Adsorption energies are in eV.

faces. Thereby we have modeled the interaction between surfaces and two common adsorbates, namely isolated H atoms and OH radicals. In particular, the calculated adsorption energy for H and OH is 6.0 and 2.9 eV at the positive, and 3.8 and 5.7 eV at the negative (0001) side, respectively. We have shown that the adsorption energy, configuration and adsorbate mobility are strongly polarization dependent, in agreement with previous experimental studies on other molecules adsorbed at the LN(0001) [9, 10]. This indicates the possibility of switching and patterning the surface chemical properties by controlling the surface ferroelectric domains.

Acknowledgements The calculations were done using grants of computer time from the Paderborn Center for Parallel Computing (PC^2) and the Höchstleistungs-Rechenzentrum Stuttgart. The Deutsche Forschungsgemeinschaft is acknowledged for financial support.

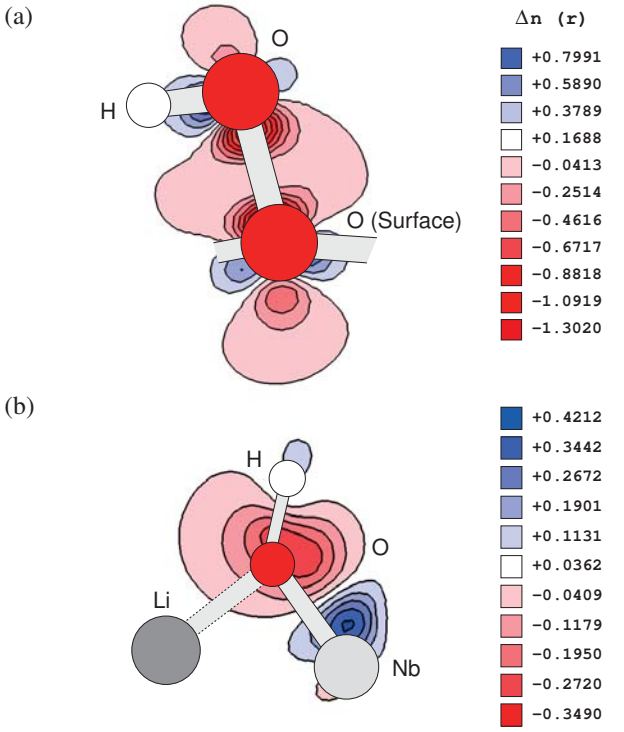

Figure 4 Charge redistribution upon adsorption of the OH radical at the positive (a) and negative (b) LN(0001) surface.

References

[1] R. S. Weis and T. K. Gaylord, Lithium-niobate - summary of physical-properties and crystal-structure, Jan 1985.
[2] W. G. Schmidt, M. Albrecht, S. Wippermann, S. Blankenburg, E. Rauls, and A. Hermann, Phys. Rev. B **77**(3) (2008).
[3] G. Namkoong, K. K. Lee, S. M. Madison, W. Henderson, S. E. Ralph, and W. A. Doolittle, Appl. Phys. Lett. **87**(17), 171107 (2005).
[4] Y. Watanabe, M. Okano, and A. Masuda, Phys. Rev. Lett. **86**(2), 332–335 (2001).
[5] W. C. Yang, B. J. Rodriguez, A. Gruverman, and R. J. Nemanich, Appl. Phys. Lett. **85**(12), 2316 (2004).
[6] B. Rosenblum, P. Bräunlich, and J. P. Carrico, Appl. Phys. Lett. **25**(1), 17 (1974).
[7] K. Nassau, H. J. Levinstein, and G. M. Loiacono, J. Phys. Chem. Solids **27**, 983 (1966).
[8] C. L. Sones, S. Mailis, W. S. Brocklesby, R. W. Eason, and J. R. Owen, J. Mater. Chem. **295**, 12 (2002).
[9] Y. Yun, L. Kampschulte, M. Li, a D. Liao, and E. I. Altman, J. Phys. Chem. C **111**, 13951–13956 (2007).
[10] J. Garra, J. M. Vohs, and D. A. Bonnell, Surf. Sci. **603**, 1106 (2009).

[11] Y. Inoue, I. Yoshioka, and K. Sato, J. Phys. Chem. **88**, 1148–1151 (1984).
[12] S. V. Kalinin, D. A. Bonnell, T. Alvarez, X. Lei, Z. Hu, J. H. Ferris, Q. Zhang, and S. Dunn, Nano Lett. **2**(6), 589–593 (2002).
[13] D. D. Fong, A. M. Kolpak, J. A. Eastman, S. K. Streiffer, P. H. Fuoss, G. B. Stephenson, C. Thompson, D. M. Kim, K. J. Choi, C. B. Eom, I. Grinberg, and A. M. Rappe, Phys. Rev. Lett. **96**(12), 127601 (2006).
[14] X. Liu, K. Kitamura, K. Terabe, H. Hatano, and N. Ohashi, Appl. Phys. Lett. **91**(4), 044101 (2007).
[15] S. Dunn and D. Tiwari, Appl. Phys. Lett. **93**(9), 092905 (2008).
[16] S. Habicht, R. J. Nemanich, and A. Gruveman, Nanotechnology(Nov), 1–4 (2008).
[17] D. Li, M. H. Zhao, J. Garra, A. M. Kolpak, A. M. Rappe, D. A. Bonnell, and J. M. Vohs, Nature Mater. **7**(6), 473 (2008).
[18] S. C. Bharath, K. R. Pimputkar, A. M. Pronschinske, and T. P. Pearl, Appl. Surf. Sci. **254**(7), 2048–2053 (2008).
[19] A. Y. Lushkin, A. Y. Lushkin, V. B. Nazarenko, V. B. Nazarenko, K. N. Pilipchak, K. N. Pilipchak, V. F. Shnyukov, V. F. Shnyukov, A. G. Naumovets, and A. G. Naumovets, J. Phys. D **32**(Jan), 9 (1999).
[20] Y. Yun, M. Li, D. Liao, L. Kampschulte, and E. Altman, Surf. Sci. **601**(19), 4636–4647 (2007).
[21] S. Sanna and W. G. Schmidt, Phys. Rev. B **81**(21), 214116 (2010).
[22] S. V. Levchenko and A. M. Rappe, Phys. Rev. Lett. **100**(25) (2008).
[23] H. Kawanowa, R. Souda, H. Ozawa, Y. Gotoh, K. Terabe, S. Takekawa, and K. Kitamura, Surf. Sci. Lett. **538**, L500–L504 (2003).
[24] J. P. Perdew and W. Yue, Phys. Rev. B **33**(12), 8800–8802 (1986).
[25] G. Kresse and J. Furthmüller, Phys. Rev. B **54**(16), 11169–11186 (1996).
[26] P. E. Blöchl, Phys. Rev. B **50**(24), 17953–17979 (1994).
[27] J. Neugebauer and M. Scheffler, Phys. Rev. B **46**(24), 16067–16080 (1992).
[28] L. Bengtsson, Phys. Rev. B **59**(19), 12301–12304 (1999).